

# Monitoring Fatigue-Induced Changes in Performance during Robot-Mediated Dynamic Movement

Kaci E. Madden, Dragan Djurdjanovic, and Ashish D. Deshpande

**Abstract**—Robotic exoskeletons are promising devices capable of both administering therapeutic exercises and assessing human movement quality. Although assessing fatigue is crucial to informing effective strategies for rehabilitation, existing metrics for evaluating fatigue during robot-mediated exercise remain underdeveloped. Current techniques focus on monitoring localized muscle fatigue, but do not consider the complex relationship between changes in muscle activity and associated alterations in joint motion during dynamic movement. In this work, we propose a system-based monitoring paradigm for tracking fatigue-induced changes in performance. The method uses a time-series model to approximate the dynamics of a human-exoskeleton system by mapping muscle activity to movement variables. An index of performance is calculated from modeling errors to continuously track changes in this dynamic relationship over time. Results showed that the index effectively captured fatigue-induced degradation in performance over time during an exoskeleton-administered resistive exercise. The index outperformed a traditional indicator of fatigue that is typically used during robotic intervention, suggesting the proposed approach has the potential to improve fatigue monitoring efforts during robot-aided movement training.

## I. INTRODUCTION

Fatigue, commonly defined as “any exercise-induced reduction in the ability of a muscle to generate force or power” [1], is a typical symptom of neurological and cerebrovascular disorders [2]. To guide effective treatment strategies for rehabilitation, assessing fatigue during therapeutic exercise is imperative [3]. Practitioners, however, are currently limited by standard clinical methods that provide qualitative metrics with low resolution, such as self-reported rating scales or questionnaires [4]. Recently, robotic interventions have enabled the development of quantitative metrics to assess movement quality by harnessing kinematic and kinetic measurements from high-resolution sensors [5]. However, the development of metrics to quantify fatigue during robot-mediated movement has garnered little attention [6]. Studies assessing fatigue during robotic interventions have focused on applying traditional signal processing techniques to analyze localized muscle fatigue, but these methods do not consider the complex relationship between muscle activity and movement that arises during dynamic contractions.

Localized muscle fatigue is frequently assessed using surface electromyography (sEMG), a non-invasive technology that records muscle electrical activity. When fatigue develops in a muscle during a sub-maximal contraction, the frequency

This work was supported in part by a NASA Space Technology Research Fellowship and internal funding at UT Austin.

K. E. Madden, D. Djurdjanovic, and A. D. Deshpande are with the Department of Mechanical Engineering, The University of Texas at Austin, Austin, TX 78712, USA [kaci.madden@utexas.edu](mailto:kaci.madden@utexas.edu)

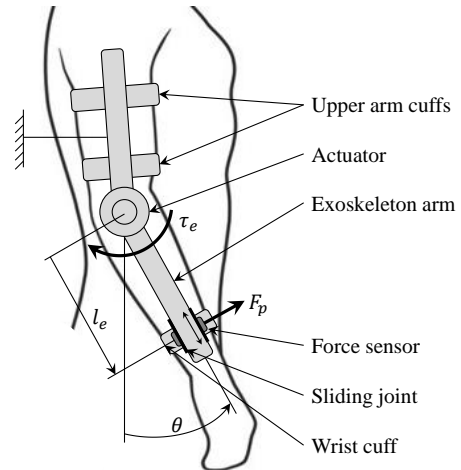


Fig. 1: Schematic of the 1-DOF exoskeleton. A subject is attached to the exoskeleton using cuffs. The position of the upper arm is fixed and the elbow is free to flex and extend. The torque applied by the exoskeleton actuator ( $\tau_e$ ) resists the subject’s movement. Joint angle ( $\theta$ ) is measured with a motor encoder. The interaction force between the human and exoskeleton ( $F_p$ ) is measured at the wrist port. The force sensor is mounted to a sliding joint located on the exoskeleton arm, whose length is  $l_e$ .

content of the sEMG signal decreases and the amplitude of the signal increases. These changes are attributed to central and peripheral nervous system mechanisms and intramuscular adaptations [7], [8], [9].

Alterations in the sEMG signal are commonly detected using traditional amplitude and frequency analyses. These methods, which are typically used to assess fatigue during robot-mediated exercise [6], [10], [11], [12], are appropriate for analyzing isometric contractions, but cannot be effectively applied to dynamic movements. Under isometric conditions, the sEMG signal can be considered wide-sense stationary over a short period of time, permitting the use of conventional Fourier-based approaches to analyzing the sEMG power spectrum. Under dynamic conditions, however, this assumption is invalid because the power spectrum changes at a much faster rate [13], [14]. Displacements in joint angle cause the position of the sEMG sensor to shift relative to the muscle fibers and the conductivity of the muscle tissue to change [14], resulting in a non-stationary sEMG signal that requires more advanced signal processing techniques to analyze. Joint time-frequency representations, such as

Cohen’s class of distributions and wavelets, have improved fatigue monitoring efforts by permitting the calculation of instantaneous amplitude and frequency parameters [13], [14]. However, variation due to changes in joint kinematics [15], [16], [17], [18], [19] are still evident in the resulting sEMG parameters.

To reduce this variation, Bonato et al. [13] proposed a method of establishing a relationship between the sEMG parameters and kinematic changes during a repetitive, cyclical task. The authors selected the most repeatable portion of the joint angle trajectory and analyzed the instantaneous frequency parameter corresponding to this region. Although the resulting sEMG parameters displayed reduced variability, this approach involved extensive post-processing. More importantly, assessing fatigue using this method would require independently analyzing one sEMG parameter per muscle, which becomes cumbersome as the number of targeted muscles increases.

In applications outside of robotics, model-based methods for relating multiple sEMG parameters to movement output have shown success in producing a single, unified metric for monitoring fatigue. Existing strategies have applied linear regression, neural networks, and correlations to map net changes in sEMG parameters to overall reductions in power [20] or force [21]. These approaches, however, are limited by their inability to continuously monitor changes in the dynamic relationship between sEMG and movement output over time. This is an important drawback given the relationship is significantly altered in the presence of fatigue [22]. The strategies are also restricted by the need for i) *a priori* assumptions that fatigue progresses linearly over time [20], ii) large data sets containing the entire time-course of fatigue to train models [20], [21], and iii) reference contractions before and after the fatiguing task [21].

A model-based approach has the potential to improve upon current fatigue assessment techniques used during robot-mediated movement, which separately evaluate changes in sEMG parameters from associated alterations in movement variables. However, the limitations of existing model-based methods must be addressed. In this work, we propose a system-based monitoring paradigm [23], [24], [25] to track fatigue-induced changes in user performance during an exoskeleton-administered dynamic task. The method approximates the dynamics of the human-exoskeleton system using a time-series model that maps instantaneous sEMG parameters to movement variables. A single performance index is then computed to continuously track changes in this dynamic relationship over time. We hypothesize that the index will capture degradation in user performance due to localized muscle fatigue and outperform a traditional indicator of fatigue based solely on sEMG that is commonly used during robot-mediated exercise.

## II. METHODS

### A. Experimental Platform: 1-DOF Exoskeleton

Our experimental platform is a single degree-of-freedom (1-DOF) exoskeleton (Fig. 1) designed to resist a human

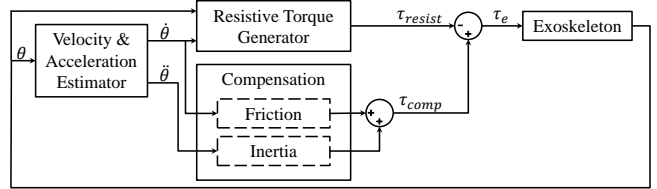


Fig. 2: Robot control. The torque generated by the exoskeleton controller ( $\tau_e$ ) consists of a prescribed resistive torque ( $\tau_{resist}$ ) and a feed-forward torque to partially compensate for the inherent impedance of the exoskeleton ( $\tau_{comp}$ ).

subject performing elbow flexion and extension. The subject’s upper arm is locked in a vertical position using two cuffs that are grounded to a rigid linkage. An additional cuff secures the subject’s wrist to the exoskeleton arm, placing the forearm in a neutral position with the palm facing medially. A linear slide rail is mounted between the wrist cuff and exoskeleton arm. This passive sliding joint compensates for small misalignments between the exoskeleton and human joint axes [26] and ensures perpendicular force application at the human wrist. Interaction forces between the human and exoskeleton,  $F_p$ , are measured with a force/torque sensor (ATI, Nano25) located between the slide rail and wrist cuff.

The exoskeleton arm and Capstan drive joint are made of Delrin acetal plastic. The transmission is composed of a brushless DC motor (Maxon, EC 60 Flat, 100 Watt) and two-stage gearing system involving a planetary gearbox (Gysin, GPL042) and Capstan drive. The motor can generate 0.3 Nm of continuous torque, features an optical incremental encoder, and operates in current mode with sinusoidal commutation by the driver (Maxon, EPOS2). The transmission ratios of the gearbox and Capstan drive are 12.25:1 and 9.85:1, respectively, producing a combined reduction ratio of 120:1.

### B. Exoskeleton Controller

We implemented an exoskeleton controller (Fig. 2) that applies resistance to the subject’s forearm with the intention of inducing muscle fatigue during movement. The torque generated by the exoskeleton controller,  $\tau_e$ , emulates an isotonic resistance training exercise and consists of a feed-forward torque,  $\tau_{comp}$ , to partially compensate for the inherent impedance of the exoskeleton and resistive torque,  $\tau_{resist}$ .

Angular velocity and acceleration are estimated from the elbow joint angle,  $\theta$ , using a double integral method with low-pass filtering [27]. The compensation torque then reduces the inherent friction and inertia of the robot. We fully compensate for Coulomb friction and partially compensate for viscous friction and inertia to ensure stability [27]. Nevertheless, the residual torque due to the remaining, unmodeled robot dynamics are accounted for in the dynamic model used for post-hoc analysis, which is described in Section II-C.

A constant resistive torque is applied in the direction opposite to the subject’s movement. The magnitude of this torque varies depending on the direction of motion since the purpose of the experiment (Section III) is to resist elbow flexion. During flexion, the prescribed load is set to 12% of

the subject's maximal elbow flexion strength ( $F_{mve}$ ). This percentage was selected based on the capacity of the exoskeleton motor. If a resistance torque is not applied during extension, the feed-forward compensation torque causes the subject to accelerate more quickly during elbow extension compared to flexion, making the cyclic movement feel unnatural. Thus, a small 2 N load is applied during extension. The combined resistive torque is calculated using the prescribed loads and moment arm,  $l_e$ , defined as the distance between the center of the exoskeleton joint axis and center of the wrist cuff (Fig. 1). To ensure smooth transitions between periods of flexion and extension, an algorithm is used to adjust the resistive torque at the extreme ranges of motion. The function records the maximum angular velocity a subject achieves during the first five flexion-extension cycles, and normalizes all subsequent velocities to this value. The normalized velocities, which range between -1 and 1, are then passed through a sigmoidal function and multiplied by the prescribed resistive torque.

### C. Dynamic Model of Coupled Human-Exoskeleton System

When the subject is attached to the robot, the coupled human-exoskeleton system can be represented by the following dynamic equation

$$(M_e + M_h)\ddot{\theta} + (b_e + b_h)\dot{\theta} + (k_e + k_h)\theta = \tau_m + \tau_p \quad (1)$$

where inertia moment ( $M_e$ ,  $M_h$ ), damping ( $b_e$ ,  $b_h$ ), and stiffness parameters ( $k_e$ ,  $k_h$ ) characterize the impedance of the exoskeleton and human, respectively. The stiffness term,  $k_h$ , is used to linearize the gravitational torque acting on the forearm, such that  $M_h g l_h \sin\theta \approx k_h \theta$  [28]. For simplicity, the coupling between the exoskeleton and human forearm is assumed to be rigid and is represented by interaction port,  $p$ , at the wrist. Accordingly, the total torque exerted on the human by the exoskeleton is denoted by  $\tau_p$ , which is calculated from  $F_p$  and  $l_e$  (Fig. 1). The parameter  $\tau_m$  approximates the net torque produced by the muscles spanning the elbow joint.

We use an autoregressive moving average model with exogenous inputs (ARMAX) to approximate (1) in a linear discrete form. The output is defined as the joint angle,  $\theta(k)$ , and the vector of system inputs is  $u(k) = [\tau_m \ \tau_p]$ . The joint torque induced by the muscles contracting,  $\tau_m$ , is modeled as a linear dynamic transformation of instantaneous features extracted from the sEMG signals.

The sEMG features are calculated using Cohen's class of time-frequency distributions (TFD) with the so-called binomial kernel [23]. The TFD, represented by  $C(t, \omega)$ , captures how the energy of the sEMG signal varies in both time,  $t$ , and frequency,  $\omega$ . Two time-frequency features representative of the instantaneous amplitude,  $\langle f^0 | t \rangle^{1/2}$ , and instantaneous mean frequency (IMNF),  $\langle f^1 | t \rangle$ , of the sEMG signal can be extracted from the zero- and first-order moments of the TFD as follows

$$\langle f^0 | t \rangle^{1/2} = \left[ \int_{-\infty}^{+\infty} C(t, \omega) d\omega \right]^{1/2} \quad (2)$$

$$\langle f^1 | t \rangle = \frac{\int_{-\infty}^{+\infty} C(t, \omega) \omega d\omega}{\langle f^0 | t \rangle} \quad (3)$$

These instantaneous features are analogous to the traditional root-mean-square amplitude [29], [30] and mean frequency [31], [8], [9] parameters, which are widely used myoelectric indicators of fatigue for isometric contractions.

The final ARMAX model for the coupled human-exoskeleton system takes the form

$$A(q)\theta(k) = B_{\tau_e}(q)\tau_e(k) + \tau_m(k) + C(q)e(k) \quad (4)$$

where

$$\tau_m(k) = \sum_{m=1}^4 \left( B_{f^0}(q) [\langle f^0 | k \rangle]_m^{1/2} + B_{f^1}(q) \langle f^1 | k \rangle_m \right) \quad (5)$$

$A$ ,  $B_{\tau_e}$ ,  $B_{f^0}$ ,  $B_{f^1}$ , and  $C$  are polynomials in the delay operator,  $q$ ,  $e(k)$  is the model disturbance considered to be zero mean Gaussian process noise,  $k$  is the sampling index for sampling interval  $T$  (i.e.  $k = kT$ ), and  $m$  is the muscle corresponding to one of four sEMG signals.

### D. Characterizing Performance Degradation

Separate ARMAX models are trained for each subject with data selected from the beginning of experiment. The data set captures an initial set of movement cycles during a repetitive flexion-extension task, prior to the subject developing significant fatigue. The trained model, referred to as the "fresh model", captures the coupled system dynamics corresponding to the subject's least degraded, or least fatigued, state. The distribution of 1-step ahead prediction errors the "fresh model" makes on the training data set is calculated and referred to as the "fresh distribution,"  $P$ . The remaining data from the experiment is partitioned into time intervals,  $T$ , that are sequentially presented to the "fresh model" to generate updated 1-step ahead prediction error distributions,  $Q_T$ . The Fidelity similarity metric [32], [33] is then calculated and used to monitor the similarity, or amount of overlap, between the "fresh distribution" and updated distributions over time. The metric, which is referred to as the Freshness Similarity Index (FSI), is defined as

$$FSI = \sum_{i=1}^N \sqrt{P(i)Q_T(i)} \quad (6)$$

where  $i$  denotes a bin of the distribution and  $N$  is the total number of bins. The FSI ranges from 0 to 1, where values near 1 indicate a high degree of similarity and those close to 0 suggest little similarity. For context, if the dynamic system remains unaltered with time, the updated distributions will be comparable to the fresh distribution. However, if the system dynamics change due to fatigue or injury, for example, the updated distribution will shift or change shape, reducing the amount of overlap with the fresh distribution. Thus, the FSI is a metric that reflects how the ARMAX approximation of the system dynamics degrades over time with respect to a normal, unfatigued state.

## III. EXPERIMENT

### A. Experimental Protocol

Four healthy, right-handed subjects participated in the study (Table I). At the start of the experiment, the subjects

TABLE I: Subject demographics, maximal voluntary contraction force ( $F_{mvc}$ ), and prescribed resistive torque ( $\tau_{resist}$ ).

Subject	Age	Gender	$F_{mvc}$ (N)	$\tau_{resist}$ (Nm)
1	27	F	136.5	3.41
2	23	M	170.9	5.11
3	20	M	152.0	4.85
4	26	F	109.1	2.72

completed three maximum voluntary isometric contractions (MVCs) separated by one minute of rest. With their elbow joint fixed ( $\theta = 90^\circ$ ), maximal elbow flexion strength,  $F_{mvc}$ , was measured using a digital force gauge (DFG55-100, Omega Engineering, Inc.). The highest  $F_{mvc}$  of the three attempts was used to calculate the resistive torque generated by the exoskeleton controller, as described in Section II-B.

Subjects then completed three sets of a dynamic task consisting of a five minute work phase followed by five minutes of rest (Fig. 3a). During the work phases, subjects performed a cyclic elbow motion against the exoskeleton-applied load. Full range of motion was defined as  $\theta = 0 - 90^\circ$  [18], and movement speed was dictated by an audible metronome set to 50 bpm. Each flexion-extension cycle consisted of two beats, resulting in an average movement frequency of approximately 0.8 Hz. Real-time visual feedback of the elbow angle was displayed on a monitor to help subjects synchronize their movement with the metronome (Fig. 3b-c). To minimize learning effects, subjects were given a warm-up trial to practice moving against an applied load in time with the metronome until they felt comfortable with the task.

### B. Data Collection

A Trigno Wireless sEMG system (Delsys Inc., Boston, MA) was used to measure muscle activity from the biceps brachii (Bic), brachioradialis (Brach), and triceps brachii long (TriLong) and lateral (TriLat) heads. Skin preparation and sEMG sensor placement (Fig. 3d) were performed according to industry standards [34]. An xPC Target (Mathworks, MATLAB module) running Simulink Real-Time was used to operate the exoskeleton in real-time and collect data at 1 kHz. The actuator and sensors (encoder, force/torque, sEMG) communicated with the target PC through data acquisition boards (National Instruments, Inc., Austin, TX.)

### C. Data Processing

Raw sEMG signals were bandpass filtered from 10 to 400 Hz using a 4<sup>th</sup> order Butterworth filter (zero-lag, non-causal) and DC offset was removed [35]. The instantaneous sEMG features were then calculated according to (2) and (3), respectively. The force/torque sensor readings were low-pass filtered using a 4<sup>th</sup> order Butterworth filter (zero-lag, non-causal) with a 6 Hz cutoff frequency to attenuate noise [36]. Prior to modeling, joint angle, torque, and sEMG feature signals were downsampled to 100 Hz.

Since the coupled human-exoskeleton system defined in (1) is represented with second-order dynamics, the autoregressive ( $A(q)$ ) and moving average ( $C(q)$ ) polynomials

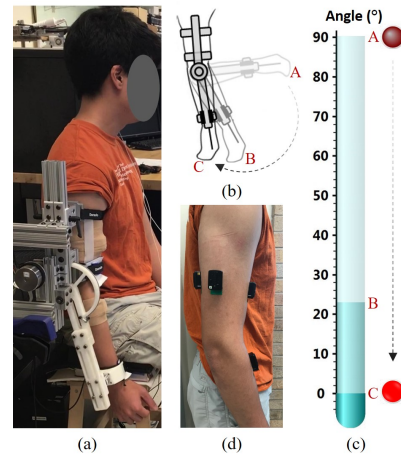


Fig. 3: Experimental setup. (a) Subject performing the cyclic dynamic task against an exoskeleton-applied resistance. (b-c) Visual feedback provided to subjects. The gauge level corresponded to the elbow joint angle. A red LED illuminated when full ROM was achieved. (d) sEMG sensor placement.

of the ARMAX model were assigned orders of 2 and 1, respectively. The order of the input polynomials  $B_{\tau_e}$ ,  $B_{f^0}$ , and  $B_{f^1}$  were determined separately for each subject by creating a range of model-order combinations and selecting the model structure that minimized the Rissanen's Minimum Description Length (MDL). For each subject, the model was trained on data taken from the initial four movement cycles of the first work phase. The amplitude of the training data set was scaled to range between 0 and 1. Fig. 4 depicts an example data set used to train the ARMAX model for a representative subject. The remaining data was normalized according to the scaling factors and partitioned into segments containing one full movement cycle, i.e., flexion followed by extension. The FSI was then calculated for each segment using (6). The slope of FSI was determined for each work phase to quantify the trend in performance degradation. An example of FSI trends are depicted in Fig. 5 for the same representative subject. Data specified in Figs. 4 and 5 were passed through a 4<sup>th</sup> order low-pass Butterworth filter with 6 Hz cutoff frequency for clarity.

A separate analysis was performed to evaluate how the local fatigue state of each muscle changed over time. Time points defining the start, middle, and end of each complete movement cycle were determined from the kinematic data and used to segment the IMNF signals into periods of flexion and extension. IMNF values were averaged over the flexion period for the flexor muscles (Bic and Brach) and the extension period for the extensor muscles (TriLong and TriLat). For each work phase, the averaged IMNF values were normalized to their mean over the initial four movement cycles. The slope of the IMNF was then calculated. A significant decreasing trend in IMNF would indicate the development of localized muscle fatigue [31], [8], [9].

Finally, a sensitivity-to-variability (SVR) metric [37] was calculated for the FSI and IMNF values from each muscle.

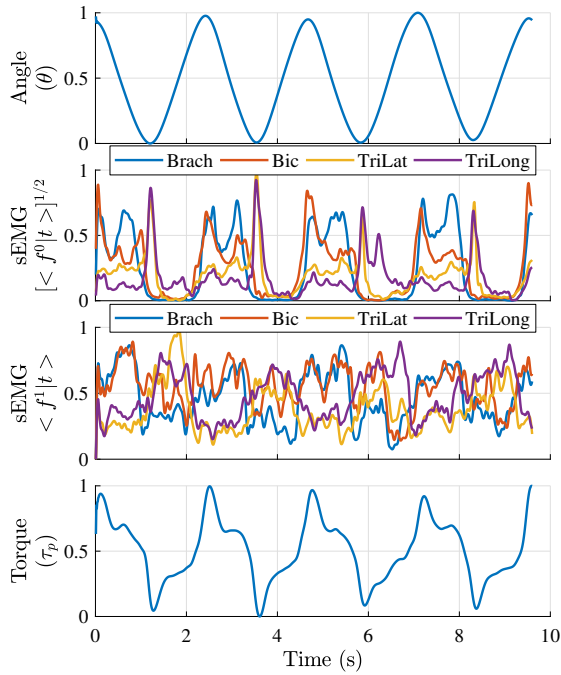


Fig. 4: Reference data set used to train the ARMAX model for Subject 1. The system output ( $\theta$ ) is presented in the top row and system inputs ( $[\langle f^0|t \rangle]^{1/2}$ ,  $\langle f^1|t \rangle$ ,  $\tau_p$ ) are shown in the bottom three rows. sEMG features (middle rows) are filtered for clarity (see text).

The metric is defined as

$$SVR = \frac{\max(\hat{I}) - \min(\hat{I})}{\sqrt{\frac{1}{P} \sum_{p=1}^P (I_p - \hat{I}_p)^2}} \quad (7)$$

where  $\hat{I}$  is the best fit line for parameter  $I$  and  $P$  is the number of estimates. The SVR relates the total decrease in the estimate of a parameter to the variability in the estimate of the parameter. This metric is used to compare the output of our system-based monitoring paradigm (FSI) to a strictly sEMG-based approach to monitoring fatigue in a single muscle (IMNF) across each work phase.

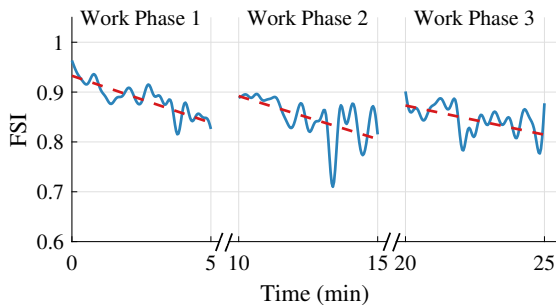


Fig. 5: FSI data from Subject 1 performing three sets of the dynamic task. FSI values are presented as solid blue lines and filtered for clarity (see text). Best-fit regression lines are shown as red dashed lines. Breaks in x-axis indicate rest.

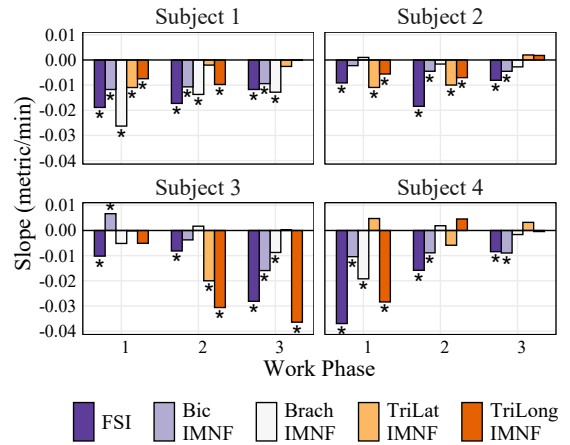


Fig. 6: Slopes of the FSI and normalized IMNF from each muscle. Stars indicate significant values ( $p < .05$ ).

#### IV. RESULTS

All subjects revealed significant negative trends in FSI over time (Fig. 6), which suggests that their performance progressively degraded during each work phase of the dynamic task. In addition, all subjects exhibited a decrease in IMNF for at least one of the elbow flexors during each work phase (Fig. 6), indicating the presence of localized fatigue in this muscle group. However, the statistical significance of the decreasing trends in IMNF varied across subjects. For Subject 1, all negative trends in both the Bic and Brach muscles achieved significance. Subject 4 displayed significant trends in at least one of the muscles for all work phases, whereas Subject 2 revealed significant decreasing trends in at least one of the flexors for the second and third work phase. Negative IMNF trends for Subject 3 reached significance for at least one elbow flexor during the third work phase. Moreover, all subjects displayed decreasing trends in IMNF for at least one of the elbow extensors during each work phase, with the exception of work phase three for Subject 2 (Fig. 6). These trends were significant in two work phases for Subjects 1, 2, and 3, and one work phase for Subject 4. Among the elbow flexor muscles, significant negative trends were more prevalent in the Bic compared to the Brach. Within the extensor muscle group, negative IMNF slopes reached significance in a larger number of work phases for the TriLong compared to the TriLat.

The SVR for the FSI was greater than the SVR from the IMNF of any muscle when averaged across subjects and work phases (Fig. 7). Considering each subject individually, the FSI displayed the highest SVR for all but one subject when averaged across work phases. For Subject 1, the FSI was only outperformed by the IMNF for the Brach.

#### V. DISCUSSION

All subjects revealed indications of localized muscle fatigue, as measured by a decrease in IMNF of the sEMG signals, during each work phase. These trends were significant for the vast majority of the work phases across subjects. In

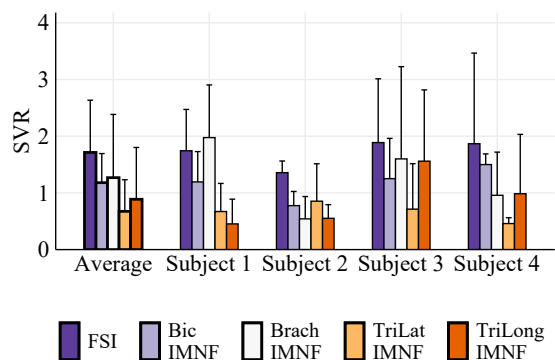


Fig. 7: Signal-to-variability ratios (SVR) of the FSI and normalized IMNF from each muscle. Bars and vertical lines represent the mean  $\pm$  1 standard deviation across work phases for Subjects 1 through 4. “Average” indicates the mean across all subjects and work phases.

some cases, however, the IMNF revealed positive trends. This could be due to a number of physiological factors, including i) the recruitment of new motor units (MUs) as contractile failure develops in those already active [7], [38], [15] and/or ii) increased MU synchronization [15] within the muscle. Since the exoskeleton controller applied a relatively small resistive torque during elbow extension, it was expected that the extensor muscles would not fatigue as much as the flexors. However, significant fatigue did occur in the triceps brachii for some subjects. This may be due to the high proportion of fast twitch muscle fibers present in the long and lateral heads of this muscle [39], [40], [41], which are known to be more susceptible to fatigue [42], [15].

All subjects revealed significant trends in FSI, indicating the relationship between their movement output and muscle activity progressively changed during the cyclic movement task. This provides sufficient evidence that the system-based monitoring paradigm successfully captured alterations in subject performance over time. The significant decreasing trends in IMNF for the majority of muscles suggests that the progressive changes captured by the FSI metric were representative of performance degradation caused by localized muscle fatigue.

The SVR considers the relationship between the long-term trend in an index (due to fatigue) and the variability about the trend (due to non-fatigue related factors). According to the SVR, the FSI outperformed the IMNF for all muscles when averaged across work phases and subjects. Given the low sample size in this study, we cannot yet claim the FSI metric is statistically superior to the IMNF using the SVR. However, it is evident that our system-based paradigm is at least comparable to an sEMG-only approach typically employed during robot-mediated exercise.

To more effectively examine how the FSI compares to other fatigue indices, including the IMNF and metrics derived from model-based methods [43], [37], future work should consider modifying the experimental protocol. The work-to-rest ratio used in this study was chosen to emulate

an exercise that could be performed during rehabilitation. However, fatigue research tends to focus on longer duration tasks performed to exhaustion [43], [6]. Tasks executed until failure will elicit greater fatigue and produce larger changes in the fatigue index, resulting in higher SVR values than those found in this study. Thus, additional experimentation should be performed to test more subjects under conditions comparable to those found in the literature.

Further research should also incorporate a “gold-standard” measure of fatigue into the experimental protocol to capture a net reduction in performance. Although this study corroborated localized-muscle fatigue using IMNF trends for individual muscles, evidence of a decline in MVC force or power output would provide confirmation that the FSI is an objective measure of fatigue, according to its well-accepted definition [1], [44]. Recent work has validated the use of a system-based approach for assessing fatigue during isometric contractions by correlating the FSI with direct measures of fatigue [45]. However, this type of analysis has yet to be performed for a dynamic movement task.

Our system-based paradigm provides advantages over a strictly sEMG-based approach to assessing fatigue during dynamic tasks that is typically used during robotic interventions. First, it effectively accounts for the inherent variability brought on by intra- and inter-individual differences and changes in joint kinematics. It does so by building a model to capture the interdependence between movement parameters and sEMG features from all involved muscles and for each subject individually. Traditional techniques that assess the IMNF of only one muscle within a group of synergists are blind to compensatory behavior that can occur in other muscles during a fatiguing task [46], [47], leaving researchers at risk of drawing false conclusions about the fatigue state of a muscle group. Moreover, factors such as age, gender, strength training experience, etc. [48], can cause considerable variation in synergistic muscle activity between individuals performing the same task [16]. Secondly, our approach effectively reduces the number of monitoring parameters to a single index, eliminating the need to separately assess changes in individual sEMG and movement parameters.

## VI. CONCLUSION

The proposed system-based monitoring paradigm, which tracks time-dependent changes in the dynamic relationship between joint kinematics, kinetics, and muscle activity, is an effective approach for assessing fatigue-induced performance changes during a robot-mediated dynamic exercise. This method offers several advantages over traditional sEMG-based strategies for monitoring fatigue during robotic interventions. Ultimately, tracking fatigue-related changes in performance has the potential to inform personalized therapeutic modalities for rehabilitation and guide the development of new control strategies for robotic movement training [49].

## ACKNOWLEDGMENT

The authors thank Job Ramirez for helping build the exoskeleton and Mira Roosth for assisting with data collection.

## REFERENCES

- [1] S. C. Gandevia, "Spinal and supraspinal factors in human muscle fatigue," *Physiological Reviews*, vol. 81, no. 4, pp. 1725–1789, Oct 2001.
- [2] M. J. Zwarts, G. Bleijenberg, and B. G. M. Van Engelen, "Clinical neurophysiology of fatigue," *Clinical Neurophysiology*, vol. 119, no. 1, pp. 2–10, 2008.
- [3] J.-S. Lou, M. D. Weiss, and G. T. Carter, "Assessment and management of fatigue in neuromuscular disease," *American Journal of Hospice and Palliative Medicine®*, vol. 27, no. 2, pp. 145–157, 2010.
- [4] T. M. Moore and E. M. Picou, "A potential bias in subjective ratings of mental effort," *Journal of Speech, Language, and Hearing Research*, vol. 61, no. 9, pp. 2405–2421, 2018.
- [5] N. Nordin, S. Q. Xie, and B. Wünsche, "Assessment of movement quality in robot-assisted upper limb rehabilitation after stroke: a review," *Journal of NeuroEngineering and Rehabilitation*, vol. 11, no. 1, p. 137, 2014.
- [6] M. Mugnosso, F. Marini, M. Holmes, P. Morasso, and J. Zenzeri, "Muscle fatigue assessment during robot-mediated movements," *Journal of NeuroEngineering and Rehabilitation*, vol. 15, no. 1, p. 119, 2018.
- [7] B. Bigland-Ritchie and J. J. Woods, "Changes in muscle contractile properties and neural control during human muscular fatigue," *Muscle & Nerve*, vol. 7, no. 9, pp. 691–699, 1984.
- [8] C. J. De Luca, "Myoelectrical manifestations of localized muscular fatigue in humans," *Critical Reviews in Biomedical Engineering*, vol. 11, no. 4, pp. 251–279, 1984.
- [9] R. Merletti, M. Knaflitz, and C. J. De Luca, "Myoelectric manifestations of fatigue in voluntary and electrically elicited contractions," *Journal of Applied Physiology*, vol. 69, no. 5, pp. 1810–1820, 1990.
- [10] A. T. Poyil, F. Amirabdollahian, and V. Steuber, "Study of gross muscle fatigue during human-robot interactions," in *The Tenth International Conference on Advances in Computer-Human Interactions. IARIA*, 2017, pp. 187–192.
- [11] J. R. Octavia, P. Feys, and K. Coninx, "Development of activity-related muscle fatigue during robot-mediated upper limb rehabilitation training in persons with multiple sclerosis: a pilot trial," *Multiple Sclerosis International*, vol. 2015, 2015.
- [12] D. Severijns, J. R. Octavia, L. Kerkhofs, K. Coninx, I. Lamers, and P. Feys, "Investigation of fatigability during repetitive robot-mediated arm training in people with multiple sclerosis," *PLOS ONE*, vol. 10, no. 7, p. e0133729, 2015.
- [13] P. Bonato, S. H. Roy, M. Knaflitz, and C. J. De Luca, "Time-frequency parameters of the surface myoelectric signal for assessing muscle fatigue during cyclic dynamic contractions," *IEEE Transactions on Biomedical Engineering*, vol. 48, no. 7, pp. 745–753, 2001.
- [14] D. Farina, "Interpretation of the surface electromyogram in dynamic contractions," *Exercise and Sport Sciences Reviews*, vol. 34, no. 3, pp. 121–127, 2006.
- [15] J. Potvin, "Effects of muscle kinematics on surface emg amplitude and frequency during fatiguing dynamic contractions," *Journal of Applied Physiology*, vol. 82, no. 1, pp. 144–151, 1997.
- [16] M. Praagman, E. Chadwick, F. Van der Helm, and H. Veeger, "The effect of elbow angle and external moment on load sharing of elbow muscles," *Journal of Electromyography and Kinesiology*, vol. 20, no. 5, pp. 912–922, 2010.
- [17] T. Kleiber, L. Kunz, and C. Disselhorst-Klug, "Muscular coordination of biceps brachii and brachioradialis in elbow flexion with respect to hand position," *Frontiers in Physiology*, vol. 6, p. 215, 2015.
- [18] K. Nakazawa, Y. Kawakami, T. Fukunaga, H. Yano, and M. Miyashita, "Differences in activation patterns in elbow flexor muscles during isometric, concentric and eccentric contractions," *European Journal of Applied Physiology and Occupational Physiology*, vol. 66, no. 3, pp. 214–220, 1993.
- [19] D. Funk, K. An, B. Morrey, and J. Daube, "Electromyographic analysis of muscles across the elbow joint," *Journal of Orthopaedic Research*, vol. 5, no. 4, pp. 529–538, 1987.
- [20] M. González-Izal, A. Malanda, E. Gorostiaga, and M. Izquierdo, "Electromyographic models to assess muscle fatigue," *Journal of Electromyography and Kinesiology*, vol. 22, no. 4, pp. 501–512, 2012.
- [21] A. C. McDonald, D. M. Mulla, and P. J. Keir, "Using emg amplitude and frequency to calculate a multimuscle fatigue score and evaluate global shoulder fatigue," *Human Factors*, vol. 61, no. 4, pp. 526–536, 2019.
- [22] J. L. Dideriksen, D. Farina, and R. M. Enoka, "Influence of fatigue on the simulated relation between the amplitude of the surface electromyogram and muscle force," *Philosophical Transactions of the Royal Society A: Mathematical, Physical and Engineering Sciences*, vol. 368, no. 1920, pp. 2765–2781, 2010.
- [23] M. Mussleman, D. Gates, and D. Djurdjanovic, "A system-based approach to monitoring the performance of a human neuromusculoskeletal system," *International Journal of Prognostics and Health Management*, vol. 7, p. 14, 2016.
- [24] Y. Y. Xie and D. Djurdjanovic, "Monitoring of human neuromusculoskeletal system performance through model-based fusion of electromyogram signals and kinematic/dynamic variables," *Structural Health Monitoring*, 2019.
- [25] K. E. Madden, D. Djurdjanovic, and A. D. Deshpande, "Monitoring human neuromusculoskeletal system performance during spacesuit glove use: A pilot study," in *Proc. IEEE Aerospace Conference*, Big Sky, MT, USA, Mar 2018, pp. 1–10.
- [26] A. Schiele and F. C. T. van der Helm, "Kinematic design to improve ergonomics in human machine interaction," *IEEE Transactions on Neural Systems and Rehabilitation Engineering*, vol. 14, no. 4, pp. 456–469, 2006.
- [27] B. Kim, A. Rodot, and A. D. Deshpande, "Impedance control based on a position sensor in a rehabilitation robot," in *Proc. ASME Dynamic Systems and Control Conference*, San Antonio, TX, USA, Oct 2014, pp. 1–7.
- [28] G. Aguirre-Ollinger, J. E. Colgate, M. A. Peshkin, and A. Goswami, "A 1-dof assistive exoskeleton with virtual negative damping: effects on the kinematic response of the lower limbs," in *2007 IEEE/RSJ International Conference on Intelligent Robots and Systems*. IEEE, 2007, pp. 1938–1944.
- [29] V. von Tschärner, "Intensity analysis in time-frequency space of surface myoelectric signals by wavelets of specified resolution," *Journal of Electromyography and Kinesiology*, vol. 10, no. 6, pp. 433–445, 2000.
- [30] B. Boashash, *Time-frequency signal analysis and processing: a comprehensive reference*, 2nd ed. Oxford: Academic Press, 2016.
- [31] J. V. Basmajian, "Muscles alive. their functions revealed by electromyography," *Academic Medicine*, vol. 37, no. 8, p. 802, 1962.
- [32] S.-H. Cha, "Comprehensive survey on distance/similarity measures between probability density functions," *International Journal of Mathematical Models and Methods in Applied Sciences*, vol. 1, no. 2, p. 1, 2007.
- [33] E. Hernández-Rivera, S. P. Coleman, and M. A. Tschopp, "Using similarity metrics to quantify differences in high-throughput data sets: application to x-ray diffraction patterns," *ACS Combinatorial Science*, vol. 19, no. 1, pp. 25–36, 2017.
- [34] H. J. Hermens, B. Freriks, R. Merletti, D. Stegeman, J. Blok, G. Rau, C. Disselhorst-Klug, and G. Hägg, "European recommendations for surface electromyography," *Roessingh Research and Development*, vol. 8, no. 2, pp. 13–54, 1999.
- [35] P. Konrad, "The abc of emg," *A Practical Introduction to Kinesiological Electromyography*, vol. 1, no. 2005, pp. 30–5, 2005.
- [36] T. E. Prieto, J. B. Myklebust, R. G. Hoffmann, E. G. Lovett, and B. M. Myklebust, "Measures of postural steadiness: differences between healthy young and elderly adults," *IEEE Transactions on Biomedical Engineering*, vol. 43, no. 9, pp. 956–966, 1996.
- [37] D. R. Rogers and D. T. MacIsaac, "Emg-based muscle fatigue assessment during dynamic contractions using principal component analysis," *Journal of Electromyography and Kinesiology*, vol. 21, no. 5, pp. 811–818, 2011.
- [38] E. A. Clancy, M. V. Bertolina, R. Merletti, and D. Farina, "Time- and frequency-domain monitoring of the myoelectric signal during a long-duration, cyclic, force-varying, fatiguing hand-grip task," *Journal of Electromyography and Kinesiology*, vol. 18, no. 5, pp. 789–797, 2008.
- [39] G. C. Elder, K. Bradbury, and R. Roberts, "Variability of fiber type distributions within human muscles," *Journal of Applied Physiology*, vol. 53, no. 6, pp. 1473–1480, 1982.
- [40] M. Johnson, J. Polgar, D. Weightman, and D. Appleton, "Data on the distribution of fibre types in thirty-six human muscles: an autopsy study," *Journal of the Neurological Sciences*, vol. 18, no. 1, pp. 111–129, 1973.
- [41] I. Kuorinka, "Restitution of emg spectrum after muscular fatigue," *European Journal of Applied Physiology and Occupational Physiology*, vol. 57, no. 3, pp. 311–315, 1988.

- [42] P. A. Tesch, "Fatigue pattern in subtypes of human skeletal muscle fibers," *International Journal of Sports Medicine*, vol. 1, no. 02, pp. 79–81, 1980.
- [43] D. T. MacIsaac, P. A. Parker, K. B. Englehart, and D. R. Rogers, "Fatigue estimation with a multivariable myoelectric mapping function," *IEEE Transactions on Biomedical Engineering*, vol. 53, no. 4, pp. 694–700, 2006.
- [44] N. K. Vøllestad, "Measurement of human muscle fatigue," *Journal of Neuroscience Methods*, vol. 74, no. 2, pp. 219–227, 1997.
- [45] K. E. Madden, D. Djurdjanovic, and A. D. Deshpande, "Using a system-based monitoring paradigm to assess fatigue during submaximal static exercise of the elbow extensor muscles," *Sensors*, vol. 21, no. 4, 2021.
- [46] N. Stutzig and T. Siebert, "Muscle force compensation among synergistic muscles after fatigue of a single muscle," *Human Movement Science*, vol. 42, pp. 273–287, 2015.
- [47] H. Akima, J. M. Foley, B. M. Prior, G. A. Dudley, and R. A. Meyer, "Vastus lateralis fatigue alters recruitment of musculus quadriceps femoris in humans," *Journal of Applied Physiology*, vol. 92, no. 2, pp. 679–684, 2002.
- [48] D. A. Neumann, *Kinesiology of the musculoskeletal system; Foundation for rehabilitation*, 2nd ed. St. Louis, Mo: Mosby/Elsevier, 2010.
- [49] L. Marchal-Crespo and D. J. Reinkensmeyer, "Review of control strategies for robotic movement training after neurologic injury," *Journal of Neuroengineering and Rehabilitation*, vol. 6, no. 1, pp. 1–15, 2009.